Cluster Extrapolation for FDD Downlink MIMO Precoding

Matthieu Roy, Stephane Paquelet, Matthieu Crussière

Cluster Extrapolation for FDD Downlink MIMO Precoding

Matthieu Roy[†], Stéphane Paquelet[†], Matthieu Crussière[‡]
[†]b<>com Rennes, France, firstname.lastname@b-com.com
[‡]Univ Rennes, INSA Rennes, IETR - UMR 6164 F-35000 Rennes, France

***Abstract*—Channel extrapolation is a promising technique to estimate the Channel State Information (CSI) in multi-input-multi-output (MIMO) systems operating in frequency division duplex (FDD) without relying on costly terminal feedback. In this paper we analyze the limits that can achieve the extrapolation of the frequency response of a propagation channel from its cluster-based representation. This method consists in measuring all the clusters characteristics (angle of departure, gain, delay) on the uplink and then extrapolating the downlink channel from those measurements. We propose a framework in which the limits of a cluster-based extrapolation process are studied taking into account delay and angular spread derived from the Saleh-Valenzuela model. We evaluate the performance of the optimal linear estimator hereby quantifying the extrapolation residual error bound in terms of Mean-Square Error and Reduction of the Beamforming Gain.**

***Index Terms*—MIMO, FDD, CSIT, Ray-based Model, Channel Reciprocity**

I. Introduction

Downlink Channel State Information (CSI) estimation is a key requirement of massive MIMO systems. To address this challenge most theoretical papers propose to use Time Division Duplex (TDD) where uplink and downlink transmissions happen on the same frequency band [1]. The downlink channel can then be directly extracted from uplink measurements. This property is called channel reciprocity.

However most currently deployed transmission systems operate in Frequency Division Duplex (FDD) where channel reciprocity doesn't hold. The user typically brings the CSI back to the base station with a feedback loop through the uplink. While this solution might be sufficient for small-scale MIMO, the overhead gets overwhelming when scaling up the dimensions of the antenna arrays.

Another strategy can be envisioned exploiting some key frequency independent features of the propagation channel. First estimated on the uplink channel, those reciprocal characteristics can be used as a prior information to reduce the overhead. For instance the main directions of departure exhibit this reciprocity property. Those have been exploited in [2]–[5] to obtain an approximate CSI used either to refine the feedback scheme or to perform simple angular precoding.

Recently, papers [6], [7] proposed to fully extrapolate the downlink channel from the uplink measurements. The principle consists in retrieving all the reciprocal parameters of a ray-based model (complex path gains, delays, directions of departure) using high resolution estimation techniques. The results were promising in the line of sight scenario that features a strong specular ray well-defined in the space-frequency domain. However it performed badly in non line of sight as the algorithm struggles to separate intra-cluster rays out of the richer multipath environment.

Indeed the multipath components that make up the propagation channel feature closely spaced rays in the space-frequency domain. Due to the finite resolution of practical antenna arrays, those intra-cluster rays remain unresolvable. This issue could be mitigated by first separating the clusters constituting the channel (for instance using high resolution techniques [6], [7]) then using frequency domain extrapolation of the frequency-dependent cluster gains.

Contributions. In this paper we investigate the theoretical limits of the extrapolation of the multipath components of a given channel in order to estimate the downlink channel from its uplink counterpart, assuming an FDD operating mode. The extrapolation error is evaluated in term of Mean Square Error and Reduction of Beamforming Gain with analytical formulas verified by numerical simulations.

We assume that the clusters constituting the multipath channel have been perfectly separated beforehand and that the long-term statistics of those clusters are perfectly known (namely the cluster delay, power, shape parameters, angular spread, directions of departure and arrival). As the clusters are characterized by a much wider coherence bandwidth than the raw channel a linear extrapolation is expected to hold on a wider frequency domain.

We perform our analysis within the framework of the well-known Saleh-Valenzuela statistical channel model described in Section II. This model has been calibrated and verified in multiple scenarios for centimeter as well as millimeter waves. The clusters constituting the channel are then decomposed on a spatial basis in Section III, on which the extrapolation process presented in Section IV relies on. Analytical extrapolation errors are derived and verified in Section V. The tensor notations introduced in this paper provide a straightforward generalization from the canonical ULA-MISO channel used in this paper up to UPAs on both sides, as presented in Section VI. Capacity loss due to the extrapolation technique is quantified in Section VII by a Reduction of Beamforming Gain approximate closed form formula.

Notations. Upper case and lower case bold symbols are used for complex matrices and vectors of arbitrary size. Curved bold symbols are used for tensors. $\langle .,. \rangle$ denote the hermitian inner product between two vectors of $\mathbb{C}^N$. $\boldsymbol{\mathcal{V}} \otimes \boldsymbol{\mathcal{W}}$ denote the tensor product between two tensor spaces. $\vec{u}$ stands for a three-dimensional (3D) vector. $\vec{a} \cdot \vec{u}$ denote the inner product between two 3D vectors. z^* denotes the conjugate of z. $[\mathbf{H}]_{p,q}$ is the element of matrix $\mathbf{H}$ at row p and column q. $\mathbf{c}[k]$ denote the k^{th} element of vector $\mathbf{c}$. $\|\mathbf{H}\|$ stands for the Frobenius norm. $\mathbf{H}^H$ and $\mathbf{H}^T$ denotes the conjugate transpose and the transpose matrices. $\mathbb{E}\{.\}$ and $\mathbb{V}\text{ar}\{.\}$ denote the expectation and variance. Throughout this paper, the indexes p, q, k, m, l denote iterators

on rays, clusters, OFDM sub-carriers, transmit antennas and angular domain basis projection coefficients, respectively.

II. MIMO Channel Model

We introduce the physically-motivated ray-based model widely used in the literature [8], [9]. In agreement with measurements, the MIMO channel is decomposed into multipath components referred to as clusters.

A. Ray-based channel model

We consider a generic MISO-OFDM channel with N_t transmit antennas, N_f subcarriers $f_1,\cdots,f_{N_f}$. Considering the plane wave assumption, we introduce the so-called *steering vector* of the antenna array $\mathbf{e_t}(\vec{u})$ defined by

$$\mathbf{e_t}(\vec{u}) = \frac{1}{\sqrt{N_t}}\left[\mathrm{e}^{-2j\pi\frac{\vec{a}_{tx,1}\cdot\vec{u}}{\lambda}},\cdots,\mathrm{e}^{-2j\pi\frac{\vec{a}_{tx,N_t}\cdot\vec{u}}{\lambda}}\right]^T \quad (1)$$

where $\vec{u}$ denotes a unit norm 3D vector indicating the direction of the ray and $\vec{a}_{tx,m}$ are 3D vectors denoting the positions of antennas in the array. We also define the *frequency domain characteristic vector* for delay τ as

$$\mathbf{e_f}(\tau) = \frac{1}{\sqrt{N_f}}\left[\mathrm{e}^{-2j\pi f_1\tau},\cdots,\mathrm{e}^{-2j\pi f_{N_f}\tau}\right]^T. \quad (2)$$

On this basis, the wideband ray-based MISO channel can be rewritten using a compact tensor formalism $\boldsymbol{\mathcal{H}} \in \mathbb{C}^{N_f}\otimes\mathbb{C}^{N_t}$ [10] as

$$\boldsymbol{\mathcal{H}} = \sqrt{N_t N_f}\sum_{p=1}^{P}\beta_p \mathbf{e_f}(\tau_p)\otimes\mathbf{e_t}^*(\vec{u}_{tx,p}). \quad (3)$$

In this model, P denote the number of rays, τ_p the arrival time of ray p. $\vec{u}_{tx,p}$ are 3D unit norm vectors denoting the direction of departure of ray p, also abbreviated DoD. The tensor notation provides a straightforward extension from this simple MISO case to any MIMO channels, as further presented in Section VI. It also provides a simple expression for the classical additive white Gaussian noise model in Einstein notation

$$\mathbf{y}_k = \boldsymbol{\mathcal{H}}_k^m \boldsymbol{\mathcal{X}}_{m,k} + \mathbf{w}_k \quad (4)$$

where the received symbols $\mathbf{y}$ are given by the transmitted symbols tensor $\boldsymbol{\mathcal{X}}$ multiplied with the tensor channel $\boldsymbol{\mathcal{H}}$ plus noise $\mathbf{w}$.

B. Clustered channel model

In practice measurement campaigns [9], [11] showed that rays are grouped into several multipath components $\mathcal{C}_q,\ q\in[1,Q]$ with similar delay, directions of departure and arrival. The clustered channel can be rewritten as

$$\boldsymbol{\mathcal{H}} = \sqrt{N_t N_f}\sum_{q=1}^{Q}\boldsymbol{\mathcal{H}_q},$$

$$\boldsymbol{\mathcal{H}_q} = \sum_{p\in\mathcal{C}_q}\beta_{p,q}\mathbf{e_f}(\tau_q+\tau_{p,q})\otimes\mathbf{e_t}^*(\vec{u}_{tx,p,q})$$

where $\tau_{p,q}$ and $\beta_{p,q}$ are the arrival time and gain of ray p in cluster q, respectively. Q denote the number of clusters, τ_q the arrival time of cluster q relatively to the first cluster. $\vec{u}_{tx,p,q}$ are 3D unit norm vectors denoting the direction of departure of ray p in cluster q, also abbreviated DoD.

C. Uniform Linear Array

Antennas are equally spaced along a straight line in a uniform linear array (ULA). We can write $\vec{a}_{tx,m} = m\vec{a}_{tx} + \vec{a}_0$ where $\|\vec{a}_{tx}\|$ is the inter-antenna spacing and $\vec{a}_0$ defines an arbitrary chosen origin point. The corresponding *steering vector* is written

$$\mathbf{e_t}(\vec{u}) = \mathbf{e_t}(\theta_{tx})$$
$$= \frac{1}{\sqrt{N_t}}\left[\mathrm{e}^{-2j\pi\left(m-\frac{N_t-1}{2}\right)\frac{\|\vec{a}_{tx}\|}{\lambda}\cos(\theta_{tx})},\ m\in[0,N_t-1]\right]^T$$

where θ_{tx} denotes the angle between vectors $\vec{a}_{tx}$ and $\vec{u}$. In the literature an equivalent steering vector expression can be found that assumes $\vec{a}_{tx,1}=0$ i.e. the first antenna is set as the origin of all the $\vec{a}_{tx,m}$ defining the array. In this paper we chose to set the centroid of the array as the origin. This notation have the advantageous property to always yield a real inner product between two steering vectors.

In the sequel we first consider a ULA transmitter. The range of our study is then extended to multiple receive antennas and UPAs in Section VI.

D. Saleh-Valenzuela model

The well-known Saleh-Valenzuela [11] model is built upon the ray-based model introduced in II-A but specifying stochastic laws for its parameters. More precisely, the times of arrivals of clusters τ_q and intra-clusters $\tau_{p,q}$ are generated by two Poisson processes of parameters Λ and λ, respectively. The ray gains $\beta_{p,q}$ follow a centered complex Gaussian distribution with variances

$$\mathbb{E}\left\{|\beta_{p,q}|^2\right\} = \mathbb{E}\left\{|\beta_{1,1}|^2\right\}\mathrm{e}^{-\tau_q/\Gamma}\mathrm{e}^{-\tau_{p,q}/\gamma}$$

where Γ and γ are the cluster decay and intra-cluster ray decay parameters respectively. $\mathbb{E}\left\{|\beta_{1,1}|^2\right\}$ is the average power of the first ray of the channel.

The directions of departure and arrival of the rays have been added latter on to model multi-antenna channels. Each cluster has an average azimuth of departure θ_q. The intra-cluster rays feature a slight azimuth offset $\Delta\theta_{p,q}$ that follows a Laplace distribution of standard deviation (also called angular spread) $\sigma_{\Delta\theta}$. Common values of $\sigma_{\Delta\theta}$ range from 5° outdoors to 26° in rich scattering indoor environments [12], [13].

E. Hypotheses

In the sequel we consider that the multipath components constituting the propagation channel have been perfectly separated. We also consider that we have a perfect knowledge of the long term statistics of the clusters, namely the cluster delay spread τ_q, the azimuth of departure θ_q, the angular spread $\sigma_{\Delta\theta}$, the decay rate γ as well as the delay rate λ. Intra-cluster delays are however too close by to be resolved, motivating a frequency-domain cluster extrapolation procedure.

III. Cluster projection

As intra-cluster rays are not resolvable, we use a Basis Expansion Model (BEM) carefully chosen to provide a sparse representation of the channel over the angular dimension. We then characterize the first and second order moments of the BEM coefficients on which the uplink to downlink extrapolation process relies on. We assume that the cluster delay is known. Without loss of generality we can set $\tau_q = 0$.

A. Angular domain projection

The main direction of cluster θ_q is already known so we can use a shifted Fourier basis designed to minimize the number of significant coefficients. More details on this approach can be found in paper [4]. The shifted Fourier basis vectors are

$$\mathbf{e_l}(\theta_q)[m] = \frac{1}{\sqrt{N_t}} \mathrm{e}^{-2\pi j\left(m-\frac{N_t-1}{2}\right)\left(\frac{l}{N_t}+\frac{\|\vec{a}_{tx}\|}{\lambda}\cos(\theta_q)\right)}.$$

In this basis the cluster tensor can be rewritten as

$$\boldsymbol{\mathcal{H}_q} = \sum_{l=0}^{N_t-1}\sum_{p=1}^{P} \alpha_{p,l,q}\mathbf{e_f}(\tau_{p,q}) \otimes \mathbf{e_l}^*(\theta_q)$$

where the coefficients $\alpha_{p,l,q}$ are given by

$$\alpha_{p,l,q} = \beta_{p,q}\langle \mathbf{e_t}(\theta_q+\Delta\theta_{p,q}), \mathbf{e_l}(\theta_q)\rangle.$$

The cluster q is then decomposed into N_t *sub-clusters* with fixed orthogonal steering vectors. The gain of each subcluster at subcarrier k, denoted $\mathbf{c_{q,l}}[k]$, can be recovered through the linear mapping

$$\mathbf{c_{q,l}} = \boldsymbol{\mathcal{H}_q}\mathbf{e_l}(\theta_q) = \sum_{p=1}^{P} \alpha_{p,l,q}\mathbf{e_f}(\tau_{p,q}).$$

Note that $\mathbb{E}\{\mathbf{c_{q,l}}\} = 0$ since the ray gains $\beta_{p,q}$ are centered.

B. Second order statistics

The inter-covariance matrix between two sub-clusters l and l' is given by

$$\mathbf{\Sigma_{q,l,l'}} = \mathbb{E}\{\mathbf{c_{q,l}}\mathbf{c_{q,l'}^H}\} = [\mathbf{\Sigma_{q,tx}}]_{l,l'}\mathbf{\Sigma_f} \tag{5}$$

where $\mathbf{\Sigma_{q,f}}$ is the covariance matrix of the equivalent SISO channel and $\mathbf{\Sigma_{q,tx}}$ is defined as

$$[\mathbf{\Sigma_{q,tx}}]_{l,l'} = \mathbb{E}_{\Delta\theta}\{\langle \mathbf{e_t}(\theta_q+\Delta\theta), \mathbf{e_l}\rangle \langle \mathbf{e_t}(\theta_q+\Delta\theta), \mathbf{e_{l'}}\rangle^*\}.$$

For a Saleh-Valenzuela cluster with parameters λ and γ the frequency covariance matrix is given by

$$[\mathbf{\Sigma_f}]_{k,k'} = P_q\left(1+\frac{\lambda\gamma}{1-2\pi j\Delta B\gamma(k'-k)}\right).$$

The proof can be found in [14]. Similarly, the coefficients of $\mathbf{\Sigma_{q,tx}}$ are given by

$$[\mathbf{\Sigma_{q,tx}}]_{l,l'} = \int_0^{2\pi} f_{\Delta\theta}(\Delta\theta) \, D_{N_t}(x_l(\Delta\theta)) D_{N_t}(x_{l'}(\Delta\theta)) d\Delta\theta \tag{6}$$

where $x_l(\Delta\theta) = \frac{l}{N_t} - \frac{\|\vec{a}_{tx}\|(\cos(\theta_q)-\cos(\theta_q+\Delta\theta))}{\lambda}$ and $D_N(x)$ denotes the Dirichlet kernel and $f_{\Delta\theta}(\Delta\theta)$ is the angular distribution of the intra-cluster rays (typically a Laplace distribution). The proof for (6) is postponed in Annex A.

C. Autocorrelation approximation

The off-diagonal elements of matrix $\mathbf{\Sigma_{q,tx}}$ are Dirichlet kernel side lobe products that are quickly negligible as N_t increase. We use the approximation that sub-clusters are uncorrelated and can be studied separately. Each sub-cluster is then fully characterized by its frequency covariance matrix $\mathbf{\Sigma_f}$ weighted by a fraction of the cluster power P_q and by $[\mathbf{\Sigma_{q,tx}}]_{l,l}$. Examples of cluster power partitioning (diagonal elements of $\mathbf{\Sigma_{q,tx}}$) over the sub-clusters are given in Fig 1. Because of the angular shift introduced in Section III-A, the first bin always represents the main direction of the cluster. As expected, more subclusters are required to model wider angular-spreads ($\sigma_{\Delta\theta}$) and broadside clusters ($\theta = 90°$).

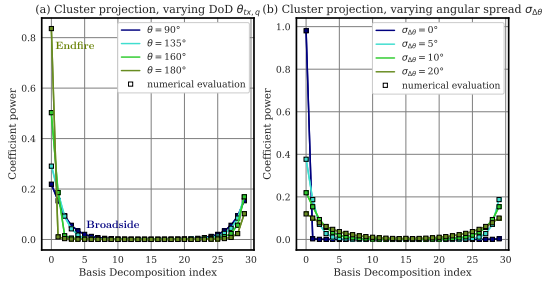

Fig. 1. Diagonal coefficients of the matrix $\mathbf{\Sigma_{q,tx}}$ for an ULA with $N_t = 30$, analytical expression (6) and numerical evaluation. On the left (a) the cluster angular spread is 10° and the cluster angle varies from 90° (broadside) to 180° (endfire). On the right (b) the angular spread of a broadside cluster varies from 0° (specular ray) to 20°.

IV. Complex gains extrapolation

As previously mentioned, subclusters can be studied separately. For ease of notation we denote any sub-cluster and its covariance matrix as

$$\begin{cases} \mathbf{c} = \mathbf{c_{q,l}} \\ \mathbf{\Sigma} = \mathbf{\Sigma_{q,l,l}}. \end{cases}$$

The subcarriers can be separated into two sets: uplink $\mathcal{U}$ and downlink $\mathcal{D}$ subcarriers. We separate the sub-cluster frequency gain vector into uplink and downlink vectors as

$$\begin{cases} \mathbf{c_u} = \mathbf{c}[k],\ k \in \mathcal{U} \\ \mathbf{c_d} = \mathbf{c}[k],\ k \in \mathcal{D}. \end{cases}$$

Our goal is to find the distribution of the downlink gains $\mathbf{c_d}$ given uplink gains measurements $\mathbf{c_u}$.

A. Sub-cluster gain modeling

We model a sub-cluster gain as a centered Wide Sense Stationary Gaussian random process with autocorrelation $\mathbf{\Sigma}$. Thermal noise and interference deteriorate the received uplink signal. Hence the measured sub-clusters are mixed with noise

$$\tilde{\mathbf{c}}_\mathbf{u} = \mathbf{c_u} + \mathbf{n}$$

with $\mathbf{n} \sim \mathcal{CN}(\mathbf{0}, \sigma_n^2\mathbf{I})$. The covariance matrix of those noisy subclusters is denoted by

$$\tilde{\mathbf{\Sigma}}_\mathbf{u} = \mathbb{E}\{\tilde{\mathbf{c}}_\mathbf{u}\tilde{\mathbf{c}}_\mathbf{u}^H\} = \mathbf{\Sigma_u} + \sigma_n^2\mathbf{I}$$

where $\mathbf{\Sigma_u}$ is the noiseless uplink covariance matrix (a submatrix of $\mathbf{\Sigma}$) and σ_n^2 denotes the noise power. We also introduce the partial covariance vectors between the uplink channel and the downlink subcarrier k denoted by

$$\boldsymbol{\sigma}_{\mathbf{u}\cup k} = \boldsymbol{\sigma}_{k\cup\mathbf{u}}^H = \mathbb{E}\{\mathbf{c_u}c_d[k]^*\}.$$

We define the downlink subcarrier variance $\sigma_k^2 = \mathbb{E}\{c_d[k]c_d^*[k]\}$. The sub-cluster gain is WSS so this variance does actually not depend on k.

The autocorrelation of the uplink channel concatenated with gain k of the downlink is given by

$$\tilde{\mathbf{\Sigma}}_{\mathbf{u}\cup k} = \begin{bmatrix} \tilde{\mathbf{\Sigma}}_\mathbf{u} & \boldsymbol{\sigma}_{\mathbf{u}\cup k} \\ \boldsymbol{\sigma}_{k\cup\mathbf{u}} & \sigma_k^2 \end{bmatrix}.$$

B. Cluster gain extrapolation

The posterior distribution of $c_d[k]$ from the noisy sub-clusters measured on the uplink $\tilde{\mathbf{c}}_\mathbf{u}$ is given after classical manipulations by

$$f_{c_d[k]|\tilde{\mathbf{c}}_\mathbf{u}}(c_d[k]|\tilde{\mathbf{c}}_\mathbf{u}) = \frac{f_{c_d[k],\tilde{\mathbf{c}}_\mathbf{u}}(c_d[k],\tilde{\mathbf{c}}_\mathbf{u})}{f_{\tilde{\mathbf{c}}_\mathbf{u}}(\tilde{\mathbf{c}}_\mathbf{u})} = \frac{|\tilde{\boldsymbol{\Sigma}}_\mathbf{u}|}{\pi|\tilde{\boldsymbol{\Sigma}}_{\mathbf{u}\cup k}|} \mathrm{e}^{-\frac{1}{\varepsilon_k^2}\left(c_d[k]-\boldsymbol{\sigma}_{\mathbf{u}\cup k}^H \tilde{\boldsymbol{\Sigma}}_\mathbf{u}^{-1}\tilde{\mathbf{c}}_\mathbf{u}\right)^2}. \quad (7)$$

$c_d[k]$ follows a complex Gaussian law, the mean of which is the Maximum a Posteriori (MAP) estimator

$$\hat{c}_d[k] = \boldsymbol{\sigma}_{\mathbf{u}\cup k}^H \left(\boldsymbol{\Sigma}_\mathbf{u} + \sigma_n^2 \mathbf{I}\right)^{-1} \mathbf{c}_\mathbf{u}$$

which is a linear estimator with variance (MSE) given by

$$\varepsilon^2[k] = \sigma_k^2 - \boldsymbol{\sigma}_{\mathbf{u}\cup k}^H \left(\boldsymbol{\Sigma}_\mathbf{u} + \sigma_n^2 \mathbf{I}\right)^{-1} \boldsymbol{\sigma}_{\mathbf{u}\cup k}. \quad (8)$$

The MSE is divided into two parts, σ_k^2 is the error without prior information and $\boldsymbol{\sigma}_{\mathbf{u}\cup k}^H \left(\boldsymbol{\Sigma}_\mathbf{u} + \sigma_n^2 \mathbf{I}\right)^{-1} \boldsymbol{\sigma}_{\mathbf{u}\cup k}$ is the accuracy gain from uplink measurements.

V. Results

In this section we provide analytical extrapolation MSE formulas for a single subcluster, verified by numerical evaluations. Those error formulas are subsequently extended to a full Saleh-Valenzuela channel.

A. Results on a single cluster

The Saleh-Valenzuela sub-cluster is parametrized by the ray arrival rate λ, the ray decay constant γ, the uplink bandwidth B_{ul}, the sub-cluster power P_q and the noise power σ_n^2. In this section we consider the normalized MSE derived from (8)

$$\frac{\mathbb{E}\{|\hat{c}_d[k]-c_d[k]|^2\}}{\mathbb{E}\{|c_d[k]|^2\}} = 1 - \frac{\boldsymbol{\sigma}_{\mathbf{u}\cup k}^H (\boldsymbol{\Sigma}_\mathbf{u} + 1/\rho \mathbf{I})^{-1} \boldsymbol{\sigma}_{\mathbf{u}\cup k}}{\sigma_k^2} \quad (9)$$

where $\rho = \frac{P_q}{\sigma_n^2}$. This expression only depends on λ, γ, B_{ul} and ρ. We introduce the dimensionless parameters $\bar{\lambda} = \lambda/B_{ul}, \bar{\gamma} = \gamma B_{ul}$. Those notations are sufficient to fully describe the cluster.

We drew the mean square error obtained for two Saleh-Valenzuela environments with $B_{ul} = 9MHz$ and 200 pilots (matches a $10MHz$ LTE frame structure). The extrapolation process works well in moderately scattered environments, such as the original Saleh-Valenzuela model [11] (Fig. 2). However the extrapolation range is much shorter in rich scattering channels such as the one described in [13] (Fig. 3) by Crabtree Building measured parameters. As expected this process works better for reduced intra-cluster scattering. The extrapolation potential of the channel also highly depends on the SNR. The process yields overall promising results at asymptotically high SNR but performances decrease rapidly in presence of thermal noise.

Using the dimensionless parameters $\bar{\lambda}, \bar{\gamma}$ we can draw the 2D map of the achievable extrapolation range for any Saleh-Valenzuela cluster on Fig. 4 at $\rho = 30dB$ for a 10% sub-cluster MSE. The extrapolation potential is given in logarithmic scale in percentages of the uplink bandwidth. We also computed the positions of characterized Saleh-Valenzuela channels of the literature [11], [13], [15] within this plane for $B_{ul} = 1MHz$ (red points) and $B_{ul} = 10MHz$ (blue points). Channels with the same characteristics but different uplink bandwidths follow straight lines with -1 slope (in log scale). A $\times 10$ bandwidth increase means $\bar{\lambda}$ is a decade decreased and $\bar{\gamma}$ a decade increased. This abacus is then very useful to compare channels and interpret the effect of a bandwidth increase.

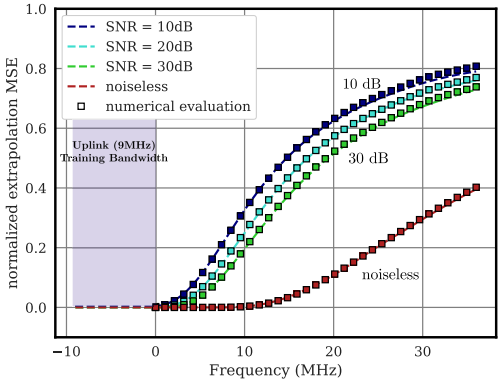

Fig. 2. Normalized MSE of the channel gain with $B_{UL} = 9MHz$ and $N_{UL} = 200$ uplink subcarriers, analytical (9) and numerical evaluation with original Saleh-Valenzuela parameters. The extrapolation scheme is very sensitive to noise.

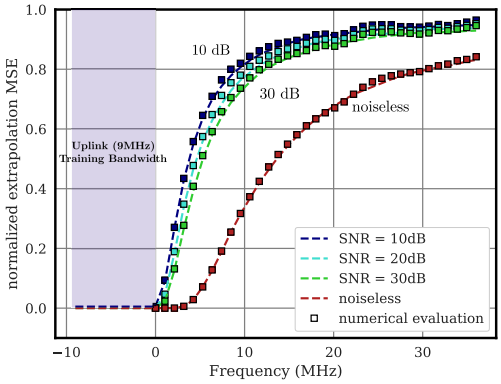

Fig. 3. Normalized MSE of the channel gain with $B_{UL} = 9MHz$ and $N_{UL} = 200$ uplink subcarriers, analytical (9) and numerical evaluation. The extrapolation scheme is very sensitive to noise. Parameters are those of [13].

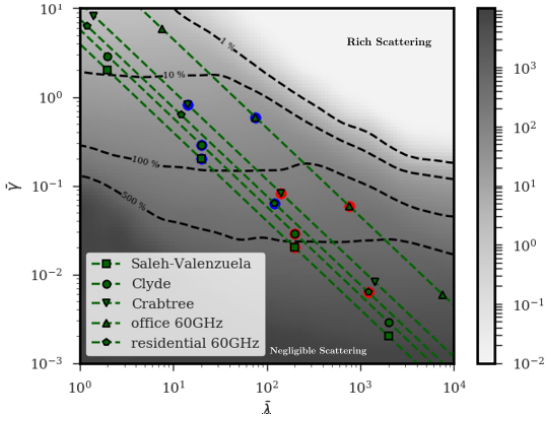

Fig. 4. Maximum achievable bandwidth extension for a single cluster (in % of the uplink bandwidth) as a function of the dimensionless cluster parameters $\bar{\lambda}$ and $\bar{\gamma}$, $\rho = 30dB$. Characterized channels have been placed onto the curve in dashed green lines (blue points: $B_{UL} = 10MHz$, red points: $B_{UL} = 1MHz$).

B. Multi-Cluster Channel

The extrapolation error is most of the time quantified by the Mean Square Error (MSE) criterion [6], [7]. The linear extrapolation approach provides a simple expression for the MSE at subcarrier k

$$\frac{\mathbb{E}\left\{\|\boldsymbol{\mathcal{H}}_k - \hat{\boldsymbol{\mathcal{H}}}_k\|^2\right\}}{\mathbb{E}\{\|\boldsymbol{\mathcal{H}}_k\|^2\}} = \frac{\sum_{q=1}^{Q}\sum_{l=0}^{N_t-1}\varepsilon_{q,l}^2[k]}{(1+\Lambda\Gamma)(1+\lambda\gamma)}$$

where $\varepsilon_{q,l}^2[k]$ is the variance of the estimated gain of subcluster l in cluster q at subcarrier k obtained from (8).

VI. Generalization

Previous results involved a transmit ULA and only one receive antenna and can be extended up to transmit and receive UPAs. In the general case the wideband channel tensor is given by

$$\boldsymbol{\mathcal{H}} = \sqrt{N_t N_f} \sum_{p=1}^{P} \beta_p \mathbf{e_f}(\tau_p) \otimes \mathbf{e_t}^*(\vec{u}_{tx,p}) \otimes \mathbf{e_r}(\vec{u}_{rx,p}). \quad (10)$$

UPA steering-vectors can be rewritten as the Kronecker product $\mathbf{e_t}^*(\vec{u}_{tx,p}) = \mathbf{e_{tx}}^*(\vec{u}_{tx,p}) \otimes \mathbf{e_{ty}}^*(\vec{u}_{tx,p})$ of two ULA steering-vectors that matches the two dimensions of the UPA. The channel tensor can be rewritten

$$\begin{aligned}\boldsymbol{\mathcal{H}} = \sqrt{N_r N_t} \sum_{p=1}^{P} \beta_p \mathbf{e_f}(\tau_p) \otimes \mathbf{e_{tx}}^*(\vec{u}_{tx,p}) \otimes \mathbf{e_{ty}}^*(\vec{u}_{tx,p}) \\ \otimes \mathbf{e_{rx}}(\vec{u}_{rx,p}) \otimes \mathbf{e_{ry}}(\vec{u}_{rx,p}).\end{aligned} \quad (11)$$

Assuming that transmit and receive arrays have dimensions N_{tx}, N_{ty} and N_{rx}, N_{ry}, each cluster is decomposed into $N_{tx}N_{ty}N_{rx}N_{ry}$ sub-clusters (most of them have a negligible power and can be neglected). As a generalization of (5), sub-clusters $\mathbf{c_{q,l_{tx},l_{ty},l_{rx},l_{ry}}}$ have the cross-cluster covariance matrix

$$\begin{aligned}\boldsymbol{\Sigma}_{\mathbf{q},\mathbf{l_{tx}},\mathbf{l'_{tx}},\mathbf{l_{ty}},\mathbf{l'_{ty}},\mathbf{l_{rx}},\mathbf{l'_{rx}},\mathbf{l_{ry}},\mathbf{l'_{ry}}} = [\boldsymbol{\Sigma}_{\mathbf{q},\mathbf{tx}}]_{l_{tx},l'_{tx}} [\boldsymbol{\Sigma}_{\mathbf{q},\mathbf{ty}}]_{l_{ty},l'_{ty}} \\ [\boldsymbol{\Sigma}_{\mathbf{q},\mathbf{rx}}]_{l_{rx},l'_{rx}} [\boldsymbol{\Sigma}_{\mathbf{q},\mathbf{ry}}]_{l_{ry},l'_{ry}} \boldsymbol{\Sigma}_{\mathbf{q},\mathbf{f}}.\end{aligned} \quad (12)$$

The same procedure can then be applied to extrapolate the subclusters. The previous formulas are still valid.

VII. Reduction of Beamforming Gain

We have shown in the previous sections that the downlink channel extrapolated from uplink measurements follows a Complex Gaussian distribution whose mean and covariance have been characterized. In this section we will use this statistical structure to derive an approximate closed form formula of the expected Reduction of Beamforming gain at subcarrier k. To that end we introduce simplified notations. $\mathbf{h}$ denotes the $N_t \times 1$ MISO channel at subcarrier k ($\mathbf{h} = \boldsymbol{\mathcal{H}}_k$). Similarly $\hat{\mathbf{h}}$ denotes the estimated MISO channel at subcarrier k ($\hat{\mathbf{h}} = \hat{\boldsymbol{\mathcal{H}}}_k$).

A. Analytical derivation of RBG

The mean square error is not the best figure of merit of an extrapolation technique. Indeed the estimated downlink channel is then used to design a precoder $\mathbf{p}$ that shapes the transmitted signal in order to optimize the capacity. In this section we use a Maximum Ratio Transmission (MRT) precoder as it yields the optimal capacity in the single user case. In multi-user cases, it has been shown that the *favorable propagation* property of massive MIMO offers a natural interference reduction mechanism. The optimal precoder is denoted

$$\tilde{\mathbf{p}} = \frac{\mathbf{h}}{\|\mathbf{h}\|}.$$

The transmitter doesn't have access to the true channel $\mathbf{h}$. It uses the estimated channel $\hat{\mathbf{h}}$ to compute the precoder

$$\tilde{\mathbf{p}} = \frac{\hat{\mathbf{h}}}{\|\hat{\mathbf{h}}\|}.$$

Capacity is the best figure of merit but is also hard to compute. Therefore most papers use intermediate metrics such as the Reduction of Beamforming Gain (RBG) [6] given by

$$RBG = \frac{|\mathbf{p}^H \mathbf{h}|^2}{|\tilde{\mathbf{p}}^H \mathbf{h}|^2}.$$

This metric is directly linked to the single-user capacity. It can be rewritten in logarithmic scale

$$RBG_{dB} \approx 10\log\left(|\mathbf{p}^H \mathbf{h}|^2\right) - 10\log\left(|\tilde{\mathbf{p}}^H \mathbf{h}|^2\right).$$

The optimal and sub-optimal beamforming gains $|\mathbf{p}^H \mathbf{h}|^2$ and $|\tilde{\mathbf{p}}^H \mathbf{h}|^2$ have similar quadratic forms structures. We introduce the Gram matrix of all sub-clusters basis functions $\mathbf{G}$ so as $[\mathbf{G}]_{l+N_t q, l'+N_t q'} = \langle \mathbf{e_l}(\theta_q), \mathbf{e_{l'}}(\theta_{q'}) \rangle$, the vector of all sub-clusters gains at subcarrier k $\mathbf{c}$ so as $\mathbf{c}_{l+N_t q} = \mathbf{c_{q,l}}[k]$ and the vector of all estimated sub-clusters gains at subcarrier k $\hat{\mathbf{c}}$ so as $\hat{\mathbf{c}}_{l+N_t q} = \hat{\mathbf{c}}_{\mathbf{q,l}}[k]$. $\boldsymbol{\mathcal{E}}$ is the diagonal covariance matrix of the channel gains $\mathbf{c}$. Taking the point of view of the transmitter, the true gains $\mathbf{c}$ are unknown. Only the distribution of $\mathbf{c} \sim \mathcal{CN}(\hat{\mathbf{c}}, \boldsymbol{\mathcal{E}})$ is known.

The inner products for optimal and sub-optimal precoding are

$$\tilde{\mathbf{p}}^H \mathbf{h} = \sqrt{N_t} \frac{\hat{\mathbf{c}}^H \mathbf{G} \mathbf{c}}{\sqrt{\hat{\mathbf{c}}^H \mathbf{G} \hat{\mathbf{c}}}} \quad \mathbf{p}^H \mathbf{h} = \sqrt{N_t} \frac{\mathbf{c}^H \mathbf{G} \mathbf{c}}{\sqrt{\mathbf{c}^H \mathbf{G} \mathbf{c}}} = \sqrt{N_t} \sqrt{\mathbf{c}^H \mathbf{G} \mathbf{c}}.$$

Their modulus squared yield the quadratic forms

$$|\tilde{\mathbf{p}}^H \mathbf{h}|^2 = N_t \frac{\mathbf{c}^H \mathbf{G} \hat{\mathbf{c}} \hat{\mathbf{c}}^H \mathbf{G} \mathbf{c}}{\hat{\mathbf{c}}^H \mathbf{G} \hat{\mathbf{c}}} = N_t \mathbf{c}^H \mathbf{A} \mathbf{c},$$
$$|\mathbf{p}^H \mathbf{h}|^2 = N_t \mathbf{c}^H \mathbf{G} \mathbf{c}.$$

According to [16], the first and second order moments are

$$\begin{cases} \mathbb{E}\{|\tilde{\mathbf{p}}^H \mathbf{h}|^2\}/N_t = \mathrm{Tr}(\mathbf{A}\boldsymbol{\mathcal{E}}) + \hat{\mathbf{c}}^H \mathbf{A} \hat{\mathbf{c}} \\ \mathbb{V}ar\{|\tilde{\mathbf{p}}^H \mathbf{h}|^2\}/N_t^2 = \mathrm{Tr}\left((\mathbf{A}\boldsymbol{\mathcal{E}})^2\right) + 2\hat{\mathbf{c}}^H \mathbf{A}\boldsymbol{\mathcal{E}}\mathbf{A} \hat{\mathbf{c}} \\ \mathbb{E}\{|\mathbf{p}^H \mathbf{h}|^2\}/N_t = \mathrm{Tr}(\mathbf{G}\boldsymbol{\mathcal{E}}) + \hat{\mathbf{c}}^H \mathbf{G} \hat{\mathbf{c}} \\ \mathbb{V}ar\{|\mathbf{p}^H \mathbf{h}|^2\}/N_t^2 = \mathrm{Tr}\left((\mathbf{G}\boldsymbol{\mathcal{E}})^2\right) + 2\hat{\mathbf{c}}^H \mathbf{G}\boldsymbol{\mathcal{E}}\mathbf{G} \hat{\mathbf{c}}. \end{cases}$$

Note that $|\tilde{\mathbf{p}}^H \mathbf{h}|^2$ follows the distribution

$$|\tilde{\mathbf{p}}^H \mathbf{h}|^2 / N_t \sim \tilde{\sigma}^2 \chi_2^2 \left(\frac{\tilde{\mu}^2}{\tilde{\sigma}^2} \right)$$

where $\tilde{\sigma}^2 = \frac{1}{2}\mathrm{Tr}(\mathbf{A}\boldsymbol{\mathcal{E}})$, $\tilde{\mu}^2 = \hat{\mathbf{c}}^H \mathbf{A} \hat{\mathbf{c}}$ and $\chi_k^2(\lambda)$ represents the noncentral Chi-Squared distribution with non-centrality parameter λ and k degrees of freedom [17].

Using the following second order approximation

$$\mathbb{E}\{f(X)\} \approx f(\mathbb{E}\{X\}) + \frac{1}{2} f''(\mathbb{E}\{X\}) \mathbb{V}ar\{X\}$$

and the previous formulas we can approximate very closely the Reduction of Beamforming Gain

$$\begin{aligned}\mathbb{E}\{RBG_{dB}\} \approx 10\log\left(\mathbb{E}\{|\mathbf{p}^H \mathbf{h}|^2\}\right) - 10\log\left(\mathbb{E}\{|\tilde{\mathbf{p}}^H \mathbf{h}|^2\}\right) \\ - \frac{5\mathbb{V}ar\{|\mathbf{p}^H \mathbf{h}|^2\}}{\ln(10)\mathbb{E}\{|\mathbf{p}^H \mathbf{h}|^2\}^2} + \frac{5\mathbb{V}ar\{|\tilde{\mathbf{p}}^H \mathbf{h}|^2\}}{\ln(10)\mathbb{E}\{|\tilde{\mathbf{p}}^H \mathbf{h}|^2\}^2}.\end{aligned} \quad (13)$$

B. Numerical experiments

We illustrate those formulas with a simple 3-clusters model with equal parameters (λ, γ, P_q), $N_t = 30$ and null angular spread. The clusters main angles are uniformly distributed $\theta_q \sim [0, 2\pi]$. As equation (13) gives the expected downlink RBG for a specific uplink realisation, both numerically evaluated and expected RGB were averaged over multiple realisations to obtain comparable results (Fig. 5). The approximation remains valid until the RGB reaches a 1.5 dB loss.

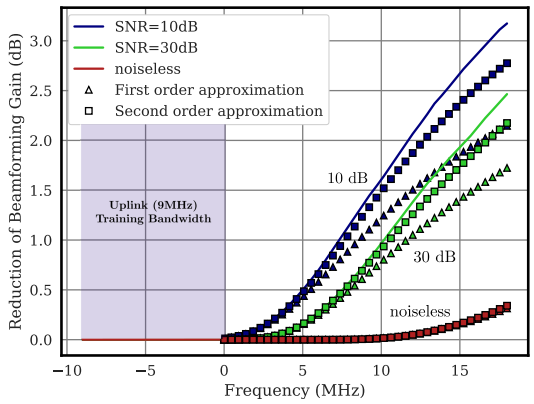

Fig. 5. Average Reduction of Beamforming Gain for 10dB, 30 dB and infinite SNR. Original Saleh-Valenzuela parameters.

VIII. Conclusion

In this paper we have investigated the limits of an extrapolation process on a wideband MIMO system to infer the downlink channel from uplink measurements. As the clusters constituting the propagation are made of a large amount of densely distributed rays that are hardly separable, a specular representation of clusters in the angular-delay domain is not available. Clusters have been projected on a adequately chosen sparse BEM in the angular domain then extrapolated in the frequency domain. Using the posterior distribution of the downlink channel, we have obtained a closed form expression for the MSE applied to Saleh-Valenzuela models. The extrapolation accuracy highly depends on both propagation channel characteristics and SNR. Cluster estimation errors for any parameters have then been summarized in a generic abacus, providing a convenient way to evaluate the extrapolation potential. We have also derived an approximate formula for the expected Reduction of Beamforming Gain.

We used the conventional MRT precoder, consistent with previous work in [6]. From the extrapolated channel distribution structure provided in this paper, new precoding strategies can however be designed to outperform MRT. On the other hand, in the last section we proposed estimates for the downlink channel gain. Those indicators could be extended to inter-user interference, providing inputs for massive MIMO resource allocation strategies.

Appendix A
Angular Second-Order Moments Derivation

For cluster q, we set the intermediary variable $x_l(\Delta\theta) = \frac{l}{N_t} + \frac{\|\vec{a}_{tx}\|}{\lambda}(\cos(\theta_q) - \cos(\theta_q + \Delta\theta))$. The inner-product between the steering vector and the basis function l yields

$$\langle \mathbf{e_t}(\theta_q + \Delta\theta), \mathbf{e_l} \rangle = \frac{1}{N_t} \sum_{m=0}^{N_t-1} \mathrm{e}^{-2\pi j (m - \frac{N_t-1}{2}) x_l(\Delta\theta)}.$$

We use the expression

$$\frac{1}{N} \sum_{m=0}^{N-1} \mathrm{e}^{jmx} = \mathrm{e}^{j\frac{N-1}{2}x} D_N(x)$$

where $D_N(x)$ denotes the Dirichlet kernel

$$D_N(x) = \frac{\sin(Nx)}{N\sin(x)}.$$

Our choice of origin in the steering vectors definition (Section II-C) cancels the phase $\mathrm{e}^{j\frac{N-1}{2}x}$ and simplify the result

$$\langle \mathbf{e_t}(\theta_q + \Delta\theta_{p,q}), \mathbf{e_l} \rangle = D_{N_t}(\pi x_l(\Delta\theta)).$$

Inserting this expression into the expectation integral yields (6).

References

[1] E. Björnson, J. Hoydis, and L. Sanguinetti, "Massive MIMO Networks: Spectral, Energy, and Hardware Efficiency," *Foundations and Trends® in Signal Processing*, vol. 11, 2017.

[2] Y. Han, J. Ni, and G. Du, "The potential approaches to achieve channel reciprocity in FDD system with frequency correction algorithms," in *Proceedings of the 5th International ICST Conference on Communications and Networking in China*, Beijing, China, 2010.

[3] D. Vasisht, S. Kumar, H. Rahul, and D. Katabi, "Eliminating Channel Feedback in Next-Generation Cellular Networks," in *Proceedings of the 2016 conference on ACM SIGCOMM 2016 Conference - SIGCOMM '16*. Florianopolis, Brazil: ACM Press, 2016.

[4] H. Xie, F. Gao, S. Zhang, and S. Jin, "A Unified Transmission Strategy for TDD/FDD Massive MIMO Systems With Spatial Basis Expansion Model," *IEEE Trans. Veh. Technol.*, vol. 66, no. 4, 2017.

[5] H. Almosa, S. Mosleh, E. Perrins, and L. Liu, "Downlink Channel Estimation with Limited Feedback for FDD Multi-User Massive MIMO with Spatial Channel Correlation," in *2018 IEEE International Conference on Communications (ICC)*. Kansas City, MO: IEEE, 2018.

[6] T. Choi, F. Rottenberg, J. Gomez-Ponce, A. Ramesh, P. Luo, J. Zhang, and A. F. Molisch, "Channel Extrapolation for FDD Massive MIMO: Procedure and Experimental Results," *arXiv:1907.11401 [cs, eess]*, 2019.

[7] F. Rottenberg, R. Wang, J. Zhang, and A. F. Molisch, "Channel Extrapolation in FDD Massive MIMO: Theoretical Analysis and Numerical Validation," *arXiv:1902.06844 [cs, math]*, 2019.

[8] L. L. Magoarou and S. Paquelet, "Parametric channel estimation for massive MIMO," *arXiv preprint arXiv:1710.08214*, 2017.

[9] T. Zwick, C. Fischer, and W. Wiesbeck, "A stochastic multipath channel model including path directions for indoor environments," *IEEE Journal on Selected Areas in Communications*, vol. 20, 2002.

[10] L. L. Magoarou and S. Paquelet, "Performance of MIMO channel estimation with a physical model," *arXiv:1902.07031 [cs, eess]*, 2019, arXiv: 1902.07031.

[11] A. A. Saleh and R. Valenzuela, "A statistical model for indoor multipath propagation," *IEEE Journal on selected areas in communications*, vol. 5, no. 2, 1987.

[12] C. Liu, E. Skafidas, and R. Evans, "Angle of arrival extended S-V model for the 60 GHz wireless indoor channel," in *2007 Australasian Telecommunication Networks and Applications Conference*. Christchurch, New Zealand: IEEE, 2007.

[13] Q. Spencer, B. Jeffs, M. Jensen, and A. Swindlehurst, "Modeling the statistical time and angle of arrival characteristics of an indoor multipath channel," *IEEE Journal on Selected Areas in Communications*, vol. 18, 2000.

[14] M. Roy, S. Paquelet, and M. Crussière, "Degrees of Freedom of Ray-Based Models for mm-Wave Wideband MIMO-OFDM (accepted)," in *2019 IEEE Global Communications Conference (GLOBECOM)*, Dec 2019.

[15] S.-K. Yong *et al.*, "G3c channel modeling sub-commitee final report," Mar. 2007.

[16] A. M. Mathai, S. B. Provost, and T. Hayakawa, *Bilinear Forms and Zonal Polynomials*, ser. Lecture Notes in Statistics. New York, NY: Springer New York, 1995, vol. 102.

[17] M. K. Simon, *Probability distributions involving Gaussian random variables: a handbook for engineers and scientists*. Springer, 2006.